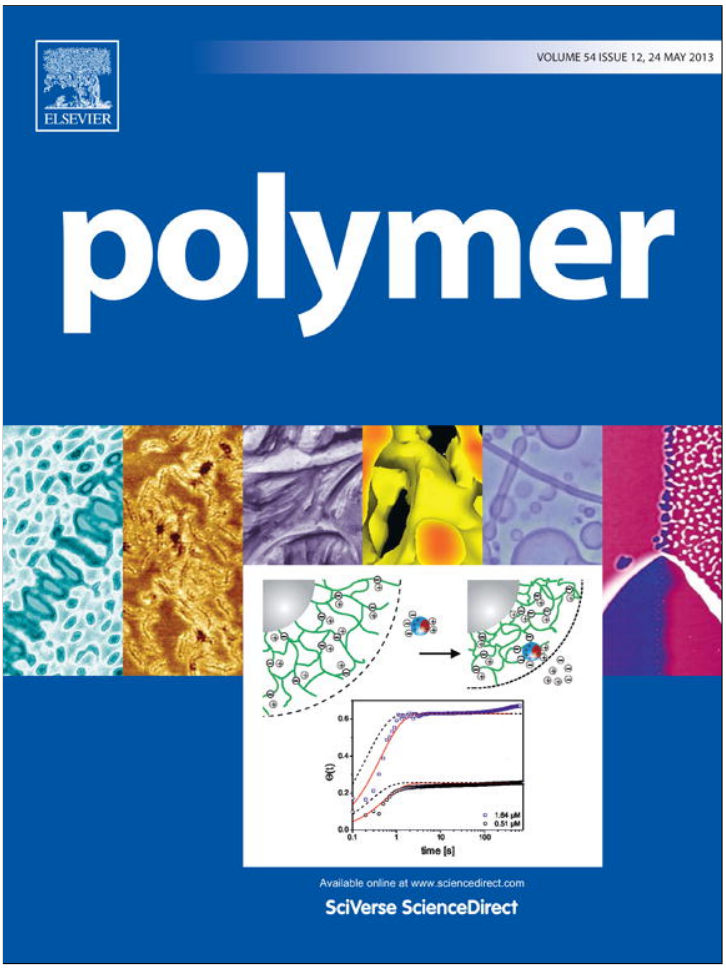

Polymer 54 (2013) 2979–2987

Contents lists available at SciVerse ScienceDirect

Polymer

journal homepage: www.elsevier.com/locate/polymer

Tough interpenetrating Pluronic F127/polyacrylic acid hydrogels

Tuba Baskan [a], Deniz C. Tuncaboylu [b], Oguz Okay [a,*]

[a] Istanbul Technical University, Department of Chemistry, 34469 Maslak, Istanbul, Turkey
[b] Bezmialem Vakif University, Faculty of Pharmacy, 34093 Istanbul, Turkey

ARTICLE INFO

Article history:
Received 22 February 2013
Received in revised form
27 March 2013
Accepted 31 March 2013
Available online 9 April 2013

Keywords:
Hydrogels
Toughness
Hydrophobic associations

ABSTRACT

Tough interpenetrating polymer network (IPN) hydrogels with pH- and temperature sensitivity were prepared by crosslinking copolymerization of acrylic acid (AAc) and N,N′-methylenebis(acrylamide) in 20 w/v% aqueous solutions of F127 (PEO_{99}-PPO_{65}-PEO_{99}). The presence of F127 within the gel network slightly decreases the elastic modulus while the loss factor significantly increases, revealing increasing energy dissipation in IPN hydrogels. Cyclic compression tests show large mechanical hysteresis in IPN hydrogels due to the reversible formation of ionic clusters and hydrophobic associations of F127 molecules. The dissipative mechanisms created by F127 lead to the improvement in the mechanical performance of IPN hydrogels when compared to the polyacrylic acid (PAAc) gel controls. PAAc hydrogel formed at 10% AAc fractures under a compression of 0.2 MPa at 78% strain, while the corresponding IPN hydrogel sustains up to 7 MPa compressions at 98% strain, leading to an increase of toughness from 31 to 335 kJ/m^3. IPN hydrogels subjected to the heating–cooling cycles between below and above the micellization temperature of F127 show characteristic features of F127 solutions, i.e., increase of the dynamic moduli on raising the temperature, and thermal hysteresis behavior.

1. Introduction

Hydrophobic interactions play a dominant role in the formation of large biological systems. These interactions can be generated in synthetic polymer systems by incorporation of hydrophobic sequences within the hydrophilic polymer chains. Aqueous solutions of hydrophobically modified hydrophilic polymers constitute a class of soft materials with remarkable rheological properties [1,2]. Above a certain polymer concentration, the hydrophobic groups in such associative polymers are involved in intermolecular associations that act as reversible breakable crosslinks creating a transient 3D polymer network. Poly(ethylene oxide) – poly(propylene oxide) – poly(ethylene oxide) (PEO-PPO-PEO) triblock copolymers, known under the trade name Pluronics, are typical amphiphilic polymers with associative properties. These copolymers may undergo thermoreversible micellization and gelation in aqueous solutions via associations of hydrophobic poly(propylene oxide) (PPO) blocks [3–8]. PPO center blocks form the core of Pluronic micelles while the relatively hydrophilic poly(ethylene oxide) (PEO) blocks forming the micelle shells interact with those of neighboring micelles [7]. As the temperature is increased, the number of Pluronic micelles also increases leading to the formation of thermoreversible hydrogels via intermicellar entanglements between PEO segments [9].

In the Pluronic family, the most extensively studied member is F127 (PEO_{99}-PPO_{65}-PEO_{99}) due to its good solubility in water and a high capacity for hydrophobic association through the relatively long PPO block. Above a certain concentration and temperature, aqueous solutions of F127 exist as spherical micelles with an aggregation number of about 50 [9,10]. The degree of overlap of the micelle shells depends on F127 concentration; at or above 18% F127, the spherical micelles pack onto a simple cubic lattice to form physical gels [9]. Pluronic F127 has attracted much attention as injectable drug delivery systems [11–14]. The sol state of F127 in aqueous solutions at room temperature facilitates incorporation of bioactive molecules, while the gel state at physiological temperature allows F127 hydrogels to serve as a drug-delivery depot. One limitation of F127 hydrogels is that they are mechanically weak and easily dissolve in physiological environments, which limit their use in load-bearing applications [13]. Several efforts have been made recently to improve the mechanical performance of F127 hydrogels [12–15]. For example, acrylate-functionalized F127 has been polymerized to obtain chemically crosslinked F127 hydrogels [16]. It was also shown that the crosslinking of F127-diacrylates in the presence of clay nanoparticles produces high-toughness nanocomposite hydrogels [17]. In ethoxysilane-capped Pluronic copolymers, the ethoxysilane groups hydrolyze over time to form

* Corresponding author. Tel.: +90 212 2853156; fax: +90 212 2856386.
E-mail address: okayo@itu.edu.tr (O. Okay).

0032-3861/$ – see front matter © 2013 Elsevier Ltd. All rights reserved.
http://dx.doi.org/10.1016/j.polymer.2013.03.066

silanol groups which covalently crosslink the copolymers [18]. Alternatively, amine-terminated Pluronics can be grafted with hyaluronic acid to form hydrogels with a reduced rate of dissolution due to the hyaluronic acid grafts [19].

In order to prevent dissolution of F127 hydrogels in aqueous media and to improve their mechanical properties, we describe here the preparation of interpenetrating polymer network (IPN) hydrogels composed of F127 and polyacrylic acid (PAAc) network chains. Thus, we apply the concept of double network (DN), first described by Gong and coworkers [20,21]. Gong's DN hydrogels were synthesized via a two-step sequential free-radical polymerization process, in which a neutral loosely crosslinked second network is incorporated within a swollen, densely crosslinked, polyelectrolyte first network. In comparison to these DN's, our IPN's consist of a physical, neutral F127 first network and a chemically crosslinked, ionic second network. More recently, DN gels with similar components as to those reported here, but with no micellization behavior have been prepared [22,23]. The design principle of the present IPN hydrogels bases on the fact that polyethers form long-lived macroradicals in the presence of radical initiators [24,25]. It was shown that the free-radical polymerization of monomers such as acrylic acid (AAc) with the chain transfer to F127 results in grafting of PAAc chains onto the Pluronic backbone [25–27]. F127-g-PAAc copolymers have unique graft-comb like structure whereby PAAc chains were attached to PPO segments of F127 via C-C bonding [24]. The graft copolymers, as linear chains or, as intramolecularly crosslinked molecules (microgels), are capable of self-assembly in response to temperature changes in aqueous media [25,26,28–30].

To obtain high-toughness IPN hydrogels with pH- and temperature-sensitive properties, we performed the free-radical crosslinking copolymerization of the AAc monomer and N,N′-methylenebis(acrylamide) (BAAm) crosslinker in aqueous 20 w/v% F127 solutions. Gelation reactions were monitored by classical rheometry using oscillatory deformation tests. The complex shear modulus G^* measured can be resolved into its real and imaginary components, i.e.,

$$G^* = G' + iG'' \tag{1}$$

where the elastic modulus G' is a measure of the reversibly stored deformation energy, and the viscous modulus G'' represents a measure of the irreversibly dissipated energy during one cycle. As will be shown below, the presence of F127 in the gelation solution significantly increases the loss factor tan δ ($=G''/G'$) indicating increase of the viscous, energy dissipating properties of the chemically crosslinked PAAc hydrogels. This increase in tan δ leads to the improvement in the mechanical performance of the resulting IPN hydrogels, as determined by uniaxial elongation and compression tests. It was also of inherent interest to investigate the viscoelastic properties IPN hydrogels in response to temperature changes between below and above the micellization temperature of F127. The results show that IPN hydrogels exhibit the characteristic features of both PAAc and F127 components.

2. Experimental part

2.1. Materials

Pluronic F127 (PEO_{99}-PPO_{65}-PEO_{99}) was purchased from Sigma–Aldrich and used without further treatment. The nominal molar mass of this copolymer is 12,600, and the weight fraction of PEO is 70%. For the rheological measurements, F127 was dissolved in water at temperatures below 10 °C for 2 h under stirring. Acrylic acid (AAc, Fluka) was freed from its inhibitor by passing through an inhibitor removal column purchased from the Aldrich Chemical Com. N,N′-methylenebis(acrylamide) (BAAm, Merck), ammonium persulfate (APS, Merck), and sodium metabisulfite (SMS, Merck) were used as received. APS and SMS stock solutions were prepared by dissolving 2.28 g APS and 1.90 g SMS separately in 10 mL of water.

2.2. Hydrogel preparation

Free-radical crosslinking copolymerization reactions of AAc and BAAm were conducted in aqueous F127 solutions at 25 °C in the presence of an APS (20 mM) − SMS (10 mM) redox initiator system. F127 concentration in the gelation solution was set to 20 w/v%. The crosslinker ratio X (mole of BAAm per mole of the monomer AAc) was also set to 1/50 while AAc concentration was varied between 5 and 30 w/v%. To illustrate the synthetic procedure, we give details for the preparation of hydrogels at an initial AAc concentration of 20 w/v%.

AAc (2.0 g) was first dissolved in 7.7 mL water at 35 °C. Then, F127 (2.0 g) was added at this temperature and stirred for 1 h to obtain a transparent solution. Note that the dissolution time of F127 was a function of AAc concentration in the solution. For example, decreasing AAc content from 2.0 to 1.0 g required around 2 h of mixing. After addition and dissolving BAAm (0.0856 g) in this solution for 30 min at 35 °C, stock solutions of SMS (0.1 mL) and APS (0.2 mL) were added to initiate the reaction. For the rheological experiments, a portion of this solution was transferred between the plates of the rheometer, while the remaining part of the reaction solution was transferred into several plastic syringes of 4 mm internal diameters. To obtain hydrogel samples in the form of sheets, the gelation solution was transferred between glass plates (20×20 cm) separated by a 1 mm Teflon spacer. The polymerization was conducted for one day at 25 °C. For comparison, hydrogels were also prepared in the absence of F127. In the following, hydrogels formed with and without F127 will be called IPN and PAAc hydrogels, respectively.

2.3. Rheological experiments

Gelation reactions were carried out between the parallel plates of the rheometer (Gemini 150 Rheometer system, Bohlin Instruments) equipped with a Peltier device for temperature control. The upper plate (diameter 40 mm) was set at a distance of 1000 μm before the onset of the reactions. During all rheological measurements, a solvent trap was used to minimize the evaporation. A frequency of 1 Hz and a deformation amplitude $\gamma_o = 0.01$ were selected to ensure that the oscillatory deformation is within the linear regime. The reactions were monitored in the rheometer at 25 °C up to a reaction time of about 3 h. After 3 h, frequency-sweep tests at $\gamma_o = 0.01$ were carried out at 25 °C over the frequency range 0. 1–40 Hz. Rheological experiments were also conducted using hydrogel samples in the form of sheets of about 150 μm thickness in their equilibrium swollen states in water. Thermal behavior of the hydrogels was investigated by heating the gel samples within the rheometer from 25 to 50 °C with a heating rate of 1 °C/min, keeping at 50 °C for 10 min, subsequently cooling down to 25 °C with a rate of 1 °C/min, and finally keeping at 25 °C for 30 min.

2.4. Gel fractions and swelling measurements

Cylindrical hydrogel samples (diameter 4 mm, length about 6 cm) were immersed in a large excess of water at 24 °C for at least 15 days by replacing water every day to extract any soluble species. The swelling equilibrium was tested by measuring the diameter of the gel samples by using an image analyzing system consisting of a microscope (XSZ single Zoom microscope), a CDD digital camera (TK 1381 EG) and a PC with the data analyzing system Image-Pro

Plus. The swelling equilibrium was also tested by weighing the gel samples. Relative volume swelling ratio V_{rel} of equilibrium swollen gels was calculated as

$$V_{rel} = (D/D_0)^3 \quad (2)$$

where D and D_0 are the swollen and initial diameters of the gel sample, respectively. Then, the equilibrium swollen gel samples were freezing dried at −40 °C/0.12 mbar for one day and −60 °C/0.01 mbar for an additional one day. The gel fraction W_g, i.e., the conversion of the monomers and F127 copolymer to the crosslinked polymer (mass of crosslinked polymer/initial mass of the monomer + F127) was calculated from the masses of dry, extracted polymer network and from the comonomer feed.

2.5. Mechanical tests

Uniaxial compression and elongation measurements were performed on hydrogel samples in the state of preparation. All the mechanical tests were performed in a thermostated room at 24 ± 0.5 °C on a Zwick Roell test machine using a 500 N load cell. For the compression tests, the cylindrical hydrogel sample of about 4 mm diameter and 3 mm length was placed between the plates of the instrument. Before the test, an initial compressive contact to 0.01 N was applied to ensure a complete contact between the gel and the plates. The tests were carried out at a constant crosshead speed of 10 and 0.3 mm min^{-1}, corresponding to a strain rate of 6×10^{-2} and 2×10^{-3} s^{-1}, respectively. Load and displacement data were collected during the experiment. Compressive stress was presented by its nominal value σ_{nom}, which is the force per cross-sectional area of the undeformed gel specimen, while the strain is given by λ, the deformation ratio (deformed length/initial length). Cyclic compression tests were conducted with a compression step performed at a constant strain rate of 6×10^{-2} s^{-1} to a maximum deformation ratio λ_{max} varied between 0.8 and 0.1, followed by immediate retraction to zero displacement, until the next cycle of compression. The stress-strain isotherms at low compression ratios were measured by using an apparatus previously described by our group [31]. Briefly, a cylindrical gel sample of about 3 mm in length was placed on a digital balance (Sartorius BP221S, readability and reproducibility: 0.1 mg). A load was transmitted vertically to the gel through a rod fitted with a PTFE end-plate. The compressional force acting on the gel was calculated from the reading of the balance. The resulting deformation was measured after 3 s of relaxation by using a digital comparator (IDC type Digimatic Indicator 543-262, Mitutoyo Co.), which was sensitive to displacements of 10^{-3} mm. The elastic or shear modulus G_o was determined from the initial slope of linear dependence:

$$\sigma_{nom} = G_o\left(\lambda - \lambda^{-2}\right) \quad (3)$$

Assuming affine network behavior, the effective crosslink density ν_e of the hydrogels was calculated from the modulus G_o at the state of gel preparation by Refs. [32,33]:

$$G_o = \nu_e RT\nu_2^0 \quad (4)$$

where $\nu_2^0$is the volume fraction of crosslinked polymer in the gel, R and T are in their usual meanings. ν_2^0 was calculated from the initial concentrations as

$$\nu_2^0 = \left(\frac{C_{F127}}{\rho_{F127}} + \frac{C_{AAc}}{\rho_{PAAc}}\right) W_g \quad (5)$$

where C_{F127} and C_{AAc} are the concentrations of F127 and AAc in the initial reaction solution, respectively (both in g/mL), and ρ_{F127} and ρ_{PAAc} are the densities of F127 (1.0 g/mL) and polyacrylic acid (1.5 g/mL), respectively.

Uniaxial elongation measurements were performed on cylindrical hydrogel samples of about 4 mm in diameter at a strain rate of 6×10^{-2} s^{-1}. The sample length between jaws was 10 ± 3 mm. For reproducibility, at least six samples were measured for each gel and the results were averaged.

3. Results and discussion

3.1. Formation and elasticity of IPN hydrogels

Free-radical crosslinking copolymerization of AAc and BAAm was carried out in 20 w/v% aqueous F127 solutions in the presence of APS-SMS redox initiator system. The crosslinker ratio was fixed at 1/50 while the initial monomer (AAc) concentration was varied between 5 and 30 w/v%. For comparison, hydrogels were also prepared in the absence of F127. In the following, hydrogels formed with and without F127 are called IPN and PAAc hydrogels, respectively. The gelation reactions were first monitored by rheometry using oscillatory deformation tests. Fig. 1A shows the elastic

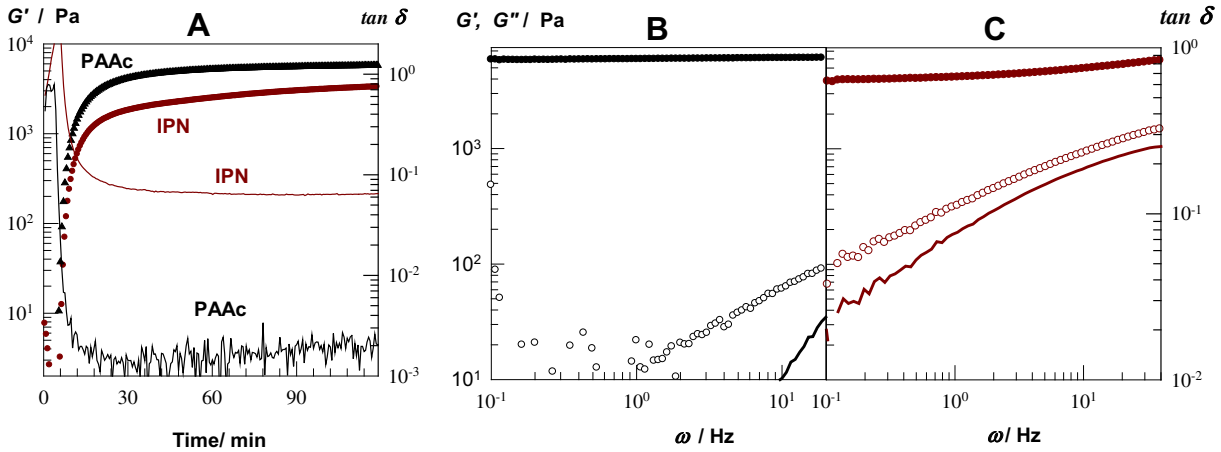

Fig. 1. A) Elastic modulus G' (symbols) and loss factor tan δ (curves) during the free radical crosslinking copolymerization of AAc and BAAm without and with 20% F127. $\omega = 1$ Hz. B, C) G' (filled symbols), G'' (open symbols) and the loss factor tan δ (curves) of PAAc (B) and IPN hydrogels (C) shown as a function of frequency ω measured after 2 h of reaction time. AAc = 10%. $X = 1/50$. Temperature = 25 °C. $\gamma_o = 0.01$.

modulus G' (symbols) and the loss factor tan δ (curves) during the reactions with 10 w/v% AAc in the feed. With or without F127, the general trend is a rapid increase of the modulus G' followed by a plateau regime after about 90 min where the modulus slightly increases. The presence of F127 in the gelation solution slightly decreases the final elastic modulus of the hydrogels while the loss factor significantly increases (from 10^{-3} to 10^{-1}). After a reaction time of 2 h, frequency-sweep tests at a strain amplitude $\gamma_o = 0.01$ were carried out over the frequency range 0.1–40 Hz. Fig. 1B and C shows the frequency dependencies of G', G'' and tan δ for PAAc and IPN hydrogels, respectively. As expected, PAAc hydrogel shows a solid-like response, i.e., G' shows a plateau over the whole frequency range while G'' remains on a low level about 2 orders of magnitude smaller than G''. This situation changes drastically for IPN hydrogels (Fig. 1C); G'' markedly increases with increasing frequency indicating that the presence of F127 creates dissipative mechanisms at the molecular level within the chemically crosslinked PAAc hydrogel. Moreover, at high frequency range, the elastic modulus G' also increases with frequency which is attributed to the entanglements between F127 and PAAc chains acting as physical crosslinks at short time scales. Thus, viscoelastic properties of the chemical PAAc hydrogel significantly change after incorporation of F127 into the gel network. Increasing AAc% in the feed from 10 to 30 w/v% also increased the elastic modulus of the hydrogels while their loss factor decreased, indicating that less energy is dissipated at high AAc contents (Fig. S1). Moreover, no gel was obtained when AAc% was decreased to 5% probably due to the extensive chain transfer reactions in the presence of F127.

Gelation reactions were also conducted in plastic syringes at 25 °C for one day to obtain gel samples with rod-shape for the gel fraction, swelling and elasticity measurements. Summary of the characteristic data of IPN and PAAc hydrogels are listed in Table 1. The incorporation of F127 into the gel network via covalent bonds was checked by the measurement of the gel fraction W_g, the mass of crosslinked, water-insoluble polymer obtained from 1 g of AAc − F127 mixture in the feed. Without F127, gel fraction W_g was equal to unity over the whole range of AAc concentration. In the presence of F127, W_g was also found to be unity at 20 and 30 w/v% AAc in the feed, indicating that all F127 molecules were incorporated into the polymer matrix via chain transfer reactions. At 10 w/v% AAc, the gel fraction W_g decreased to 0.6; assuming that the conversion of AAc to the crosslinked polymer is complete, this means that about 40% of F127 in the gelation solution become part of the hydrogel network at this AAc concentration.

Table 1 also shows that the shear modulus G_o of IPN hydrogels is smaller than PAAc hydrogels over the whole range of AAc content. Assuming affine network behavior, the effective crosslink densities ν_e calculated using Eq. (4) are shown in Table 1 and Fig. 2A. IPN hydrogel exhibits a lower effective crosslink density as compared to the corresponding PAAc hydrogel formed in the absence of F127 molecules. This reduction in ν_e may be attributed to the steric effect of F127 on the gelation kinetics of vinyl-divinyl monomer copolymerization [34]. Thus, F127 molecules attached to the growing PAAc chain radicals during gelation may reduce the reactivity of the pendant vinyl groups to form effective crosslinks. Moreover, formation of shorter primary chains due to the chain transfer to F127 may also be responsible for this behavior. Since the lower the crosslink density, the higher the swelling ratio, one may expect a higher degree of swelling of IPN hydrogels as compared to PAAc hydrogels. However, an opposite behavior was observed as illustrated in Fig. 2B where the equilibrium swelling ratios V_{rel} of the hydrogels are plotted against pH of the external solution. Although IPN hydrogels are less crosslinked, they exhibit a lesser degree of swelling at pH < 9 as compared to the corresponding PAAc hydrogels. This finding is in accord with a recent report indicating that the swelling degree of PAAc gel decreases with increasing F127 content [35].

We attribute this behavior to the decrease of the dissociation degree of AAc units in the network chains due to the presence of F127 molecules. Bromberg et al. indeed observed that pK_a of F127-g-PAAc microgels is larger than pK_a of PAAc [36]. This difference in pK_a was explained by the formation of hydrophobic associations between PPO segments of the microgels in aqueous solutions [36]. Such associations alter electrostatic charge density and the availability of the carboxyls on the PAAc chains to neutralization, which may lead to a decrease in the swelling ratios of the hydrogels containing F127. However, at high pH, increasing degree of ionization of AAc units also increases the osmotic pressure exerted by the mobile counterions leading to the weakening of the hydrophobic associations and to gel swelling. This was supported by the fact that at pH > 9, IPN hydrogels swell more than PAAc gels due to their lower crosslink densities (Fig. 2B).

3.2. Mechanical properties of the hydrogels

Fig. 3 compares stress–strain data of IPN and PAAc hydrogels, as the dependence of the nominal stress σ_{nom} on the deformation ratio λ in compression ($\lambda < 1$) and elongation tests ($\lambda > 1$). IPN hydrogels (solid curves) exhibit a higher strain at break and a higher degree of toughness when compared to the PAAc gel controls (dashed curves). For example, PAAc hydrogel formed at 10 w/v % AAc fractures under a compression of 0.2 MPa at 78% strain while the corresponding IPN hydrogel sustains up to 7 MPa compressions at 98% strain, leading to an increase of toughness from 31 to 335 kJ/m^3. The improvement in the mechanical performance of IPN hydrogels is due to the increased associativity in the gel network so that more energy is dissipated under deformation at large strains. In Fig. 4, the compressive stress–strain curves of IPN and PAAc hydrogels are given at two different strain rates. For PAAc hydrogels, the compression ratio at break and the compressive strength are independent on the strain rate in the range investigated, while in IPN hydrogels, they both increase as the strain rate is increased. These results highlight the dynamic properties of IPN hydrogels and in accord with the rheological test results. As seen in Fig. 1C, tan δ of IPN hydrogel remarkably increases with raising frequency revealing that the elastic nature of the hydrogel decreases and more energy dissipation occurs at short experimental time scales. This increase in energy dissipation at short times is reflected in Fig. 4 by enhanced toughness of IPN hydrogels at high strain rates.

The large strain properties of IPN and PAAc hydrogels were compared by cyclic compression tests conducted up to a strain below the failure. The tests were conducted by compression of cylindrical gel samples at a strain rate of 6×10^{-2} s^{-1} to a predetermined maximum compressive strain value λ_{max}, followed by immediate retraction to zero displacement [37,38]. In both IPN and PAAc hydrogels, the loading curve of the compressive cycle was different from the unloading curve indicating damage in the gels and dissipation of energy during the cycle. In Fig. 5A, two

Table 1
Characteristics of IPN and PAAc hydrogels. m_{AAc}/m_{F127} = mass ratio of AAc to F127 in the feed for IPN hydrogels. W_g = gel fraction G_o = shear modulus after gel preparation, ν_e = effective crosslink density of the hydrogels. (Standard deviations in parentheses).

AAc%	m_{AAc}/m_{F127}	W_g		G_o/kPa		ν_e/mol m^{-3}	
		IPN	PAAc	IPN	PAAc	IPN	PAAc
10	0.5/1	0.6 (0.1)	1.0	4.0 (0.5)	8.6 (0.2)	10 (1)	52 (1)
20	1.0/1	1.0	1.0	48 (4)	60 (4)	59 (5)	183 (12)
30	1.5/1	1.0	1.0	105 (4)	115 (5)	106 (4)	233 (10)

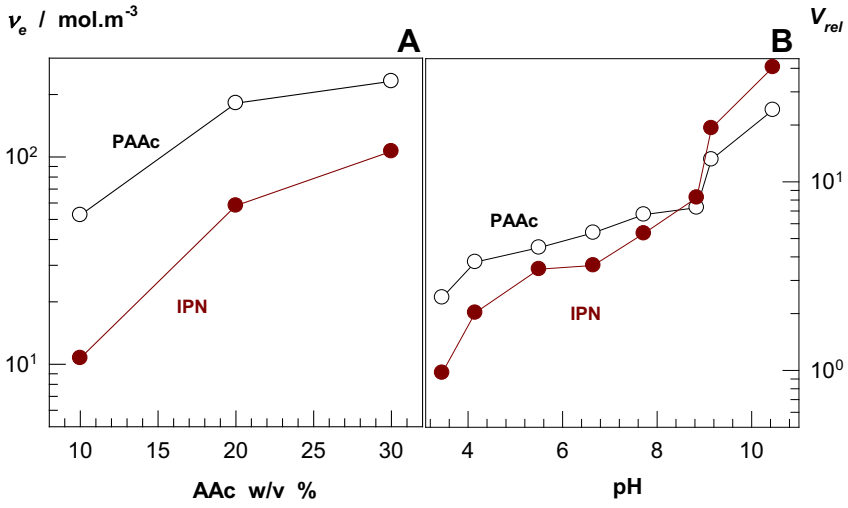

Fig. 2. A) Effective crosslink density ν_e of PAAc and IPN hydrogels shown as a function of AAc content in the monomer feed. B) Relative volume swelling ratios V_{rel} of PAAc and IPN hydrogels plotted against pH of the external solutions. AAc = 10 w/v%. X = 1/50. Temperature = 25 °C.

successive loading–unloading cycles to $\lambda_{max} = 0.1$ are shown for an IPN hydrogel sample formed at 10 w/v% AAc. The perfect superposition of the successive loading curves demonstrates that the damage done to the gel sample during the loading cycle is recoverable in nature. The reversibility of loading/unloading cycles was observed in all gel samples with or without F127. This suggests the existence of reversible breakable bonds in both PAAc and IPN hydrogels.

Fig. 5B shows typical results of the loading/unloading experiments of IPN hydrogels with increasing maximum strain from 50 to 90% (λ_{max} = 0.5 to 0.1). The energy U_{hys} dissipated during the compression cycle was calculated from the area between the loading and unloading curves. In Fig. 5C, the hysteresis energy U_{hys} for IPN (filled symbols) and PAAc hydrogels (open symbols) is plotted against the reduced deformation ratio λ_{red}, defined as

$$\lambda_{red} = \frac{1-\lambda}{1-\lambda_b} \tag{6}$$

where λ_b is the deformation ratio at failure. According to Eq. (6), λ_{red} = 0 and 1 for gels in the undeformed state and at the deformation to break, respectively so that all hysteresis data of the hydrogels are presented in Fig. 5C in the same deformation scale. It is seen that the hysteresis energy U_{hys} at large strains is much larger in IPN hydrogels as compared to PAAc hydrogels. Because U_{hys} can

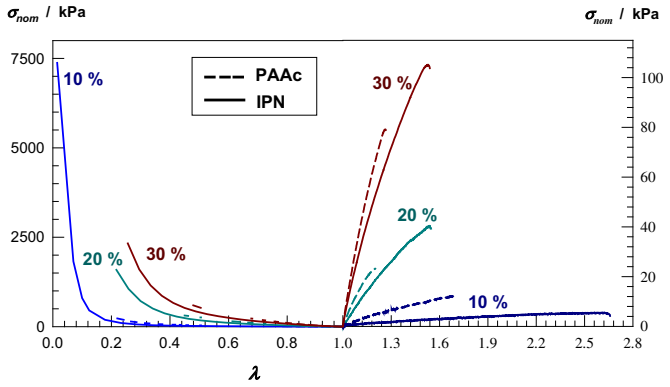

Fig. 3. Stress–strain curves of IPN (solid curves) and PAAc hydrogels (dashed curves) under elongation ($\lambda > 1$) and compression ($\lambda < 1$). AAc w/v% in the feed as indicated. Strain rate = 6×10^{-2} s^{-1}.

be interpreted as the dissociation energy of physical bonds broken down during the compression cycle [37,38], this reveals existence of a larger number of such physical bonds in IPN hydrogels. In PAAc hydrogels with negligible viscous properties (Fig. 1B), the appearance of hysteresis is due to the reversible formation of ionic clusters under large strain, as identified recently [39,40]. In IPN hydrogels, U_{hys} is much larger due to the presence of both ionic clusters and hydrophobic associations of F127 molecules. Thus, the larger number of breakable bonds in IPN hydrogels is responsible for their enhanced mechanical properties.

3.3. Thermal behavior of the hydrogels

The thermal behavior of IPN hydrogels was investigated by subjecting the gel samples to heating–cooling cycles between 25 and 50 °C, during which the dynamic moduli of the gels were monitored as a function of temperature. For comparison, we first investigated the thermal behavior of 20 w/v% F127 solution during this cycle. Fig. 6A shows the variations of G' (filled circles), G'' (open circles) and tan δ (filled triangles) of F127 solution during the course of the heating and cooling periods. In Fig. 6B, the frequency dependence of G' and G'' of this solution at 25 and 50 °C as well as, after cooling back to 25 °C is shown. Before heating, the solution at 25 °C shows a liquid like response, i.e. G'' exceeds G' over the whole range of frequencies investigated, indicating that F127 chains in the solution mainly exist as unimers. This is reasonable because water at this temperature is a good solvent for both PPO and PEO blocks of F127 [9]. During heating of the solution and particularly between 28 and 33 °C, both moduli rapidly increase and, gelation occurs at 28 °C as evidenced by the decrease of the loss factor tan δ below unity. Moreover, G'' increases faster than G' in the transition region resulting in the appearance of a maximum in tan δ versus temperature plot. Gelation of F127 solution is due to the increased hydrophobicity of PPO blocks with rising temperature, leading to the destruction of the cage like water structure surrounding F127 molecules. This dehydration of F127 leads to the formation of spherical micelles with PPO blocks forming the core surrounded by a shell of PEO blocks [9]. As the temperature is increased, the number of the micelles also increases making the intermicellar distances shorter so that the intermicellar entanglements acting as physical crosslinks lead to F127 gelation. More than 4 orders of magnitude increase of the elastic modulus during heating suggest the existence of a significant number of such entanglements

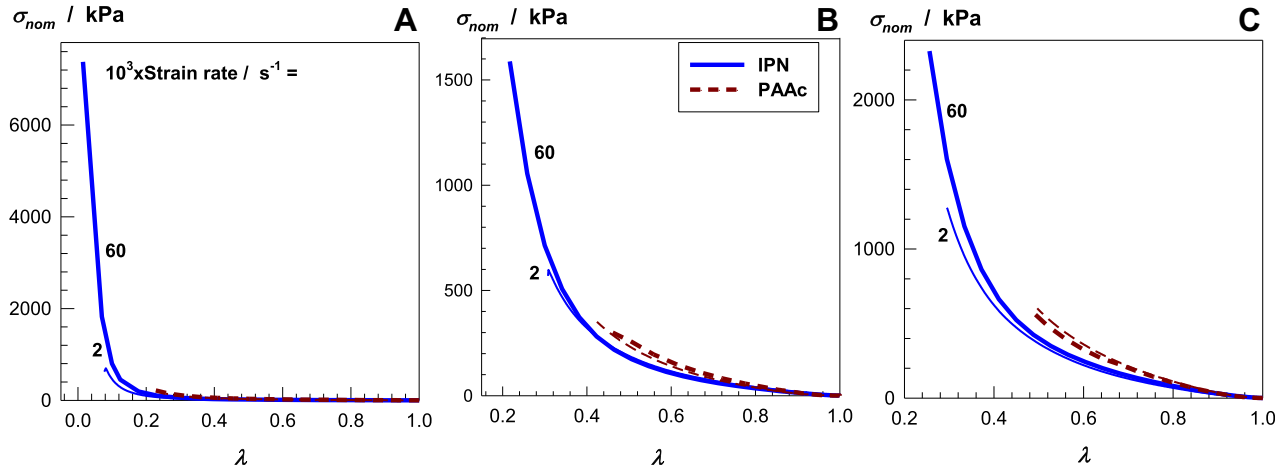

Fig. 4. Compressive stress–strain curves of IPN (solid curves) and PAAc hydrogels (dashed curves). Strain rate = 6×10^{-2} s^{-1} (thick curves) and 2×10^{-3} s^{-1} (thin curves). AAc in the feed = 10 (A), 20 (B), and 30 w/v% (C).

serving as crosslinks at the time scale of the experiments (about 0.2 s). Moreover, the fact that the viscous modulus also increases significantly in the same range of temperature reveals that the intermicellar frictions of close packed F127 micelles significantly contribute to their viscous behavior.

Fig. 6A and B also shows that the sol–gel transition phenomenon of 20% F127 solution is not reversible, i.e., at the end of the heating–cooling cycle, the system does not return to its initial state and remains as an elastic F127 mesh. For example, at $\omega = 1$ Hz, the solution exhibits an elastic modulus of 5 kPa after the heating–cooling cycle compared to its initial value of 0.08 Pa. At the same time, the viscous modulus of this sample also increases from 0.5 to 600 Pa and, both G' and G'' become frequency-independent after the cycle (Fig. 6B). Such a large hysteresis was reported recently for Pluronic F108 (PEO_{133}-PPO_{50}-PEO_{133}) as well as for polyglycidol-PPO-polyglycidol triblock copolymers in concentrated aqueous solutions [7,41]. This behavior is mainly attributed to the slow relaxation of intermicellar entanglements due to the high viscosity of the solution [7]. Since F127 concentration used in the present study (20%) is much larger than the cmc value of F127 at 25 °C (~0.7%), one may expect that the gel of close packed F127 micelles formed at a high temperature cannot reorganize to form the initial conformation upon cooling back to 25 °C. A similar behavior was observed in semi-dilute aqueous solutions of double-stranded DNA subjected to heating–cooling cycles between below and above the DNA denaturation temperature [42].

IPN hydrogels were also subjected to the same heating–cooling cycle. Fig. 7 shows the variations of G', G'' and tan δ of IPN hydrogel with 10 w/v% AAc plotted against the temperature during heating from 25 to 50 °C. For comparison, the behavior of the corresponding PAAc hydrogel sample is also shown in the figure by the open symbols. The viscous modulus G'' and tan δ of PAAc hydrogel remain almost unchanged over the whole temperature range while its elastic modulus G' slightly increases due to entropic effects. In contrast, the dynamic moduli of IPN hydrogel significantly increase with rising temperature indicating that the addition of F127 generates temperature sensitivity in PAAc gels. All IPN hydrogels exhibited temperature sensitivity with an increase in the dynamic moduli on rising the temperature, revealing formation of hydrophobic associations within the gel network (Fig. S2). The temperature sensitivity of IPN hydrogels was also observed after their equilibrium swelling in water (Fig. S3). As compared to F127

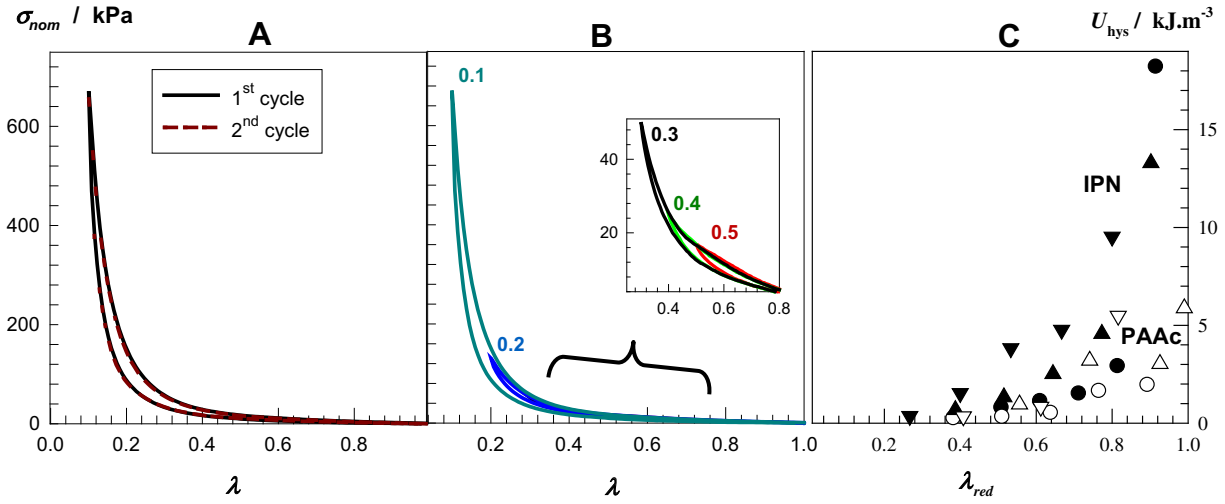

Fig. 5. (A, B): Stress σ_{nom} vs. deformation ratio λ curves from cyclic compression tests for the gel samples formed at 10 w/v% AAc. Strain rate = 6×10^{-2} s^{-1}. (A): Two successive loading/unloading cycles for a maximum compressive strain $\lambda_{max} = 0.1$. (B): Loading/unloading cycles with increasing strain from $\lambda_{max} = 0.5$ to 0.1, as indicated. (C): Hysteresis energy U_{hys} shown as a function of the reduced strain λ_{red} for IPN (filled) and PAAc hydrogels (open symbols). AAc = 10 (circles), 20 (triangles up), and 30 w/v % (triangles down).

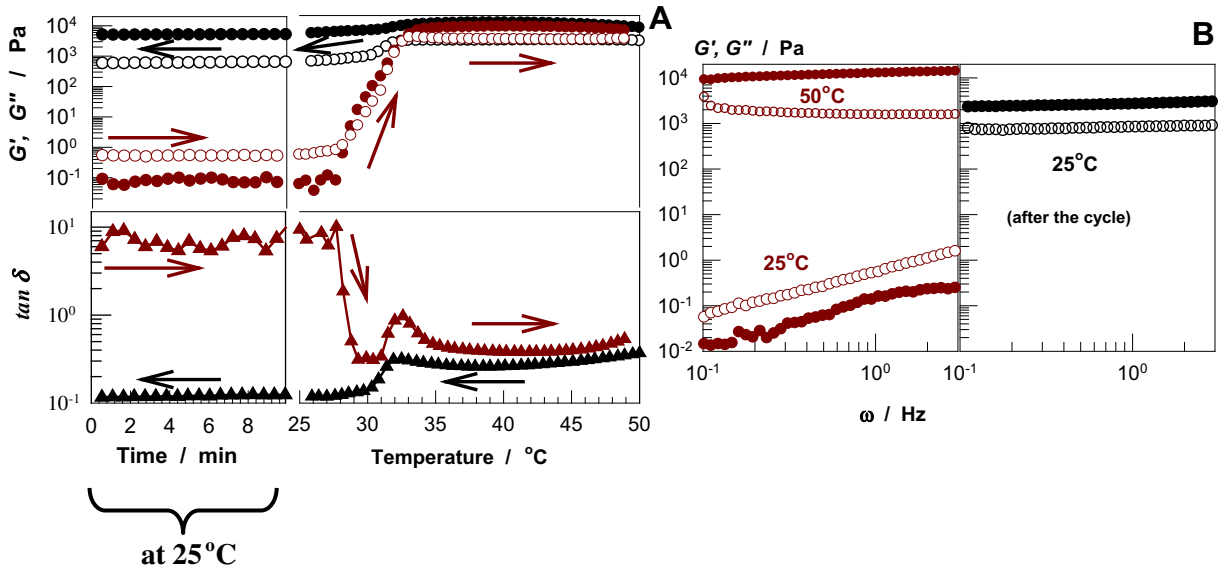

Fig. 6. A) G' (filled circles), G'' (open circles), and tan δ (filled triangles) of 20% F127 solution during the heating–cooling cycle between 25 and 50 °C. The arrows indicate the direction of the temperature change. $\omega = 1$ Hz. $\gamma_o = 0.01$. B) G' (filled symbols) and G'' (open symbols) of 20% F127 solution as a function of frequency ω at temperatures indicated. $\gamma_o = 0.01$.

solution, the extent of the moduli variations is however limited due to the crosslinked network structure and, due to the structural constraints to F127 segments by the attached PAAc network chains. Moreover, the irreversible thermal response of 20% F127 solution was also observed in IPN hydrogels. In Fig. 8, the variations of G', G'', and tan δ of IPN hydrogels are shown during the heating and cooling periods. Similar to the behavior of F127 solutions (Fig. 6A), IPN hydrogels after the cycle exhibit larger dynamic moduli as compared to the virgin gel samples. Moreover, the loss factor attains larger values after the cycle indicating increasing viscous properties of IPN hydrogels subjected to heating–cooling cycle.

According to the theory of rubber elasticity, the network mesh size ξ of IPN hydrogels can be estimated from the number of repeat units between successive chemical crosslinks, N, by Ref. [43]:

$$\xi = aN^{0.5}\left(v_2^0\right)^{\frac{-1}{3}} \tag{7}$$

where a is the bond length ($1.5A_o$). Since the effective length N of the network chains is related to the crosslink density ν_e by: [32,33]

$$N = (\nu_e V_r)^{-1} \tag{7a}$$

where V_r is the molar volume of the repeat unit (48 mL/mol), a rough estimate gives the mesh size ξ as 12, 4, and 3 nm, for IPN hydrogels with 10, 20, and 30% AAc, respectively. On the other hand, the hydrodynamic radius of free F127 micelles was estimated to be about 10 nm [9]. In concentrated solutions such as those in the present study, the micelle shells are partially overlapped while the core radius remains unchanged at 4.1 nm [9]. Thus, despite the structural constraints due to the attached PAAc segments, we may speculate that the temperature-dependent micellization of F127 is possible in the IPN hydrogel with 10% AAc in the feed. As illustrated in Fig. 9, F127 initially exists as unimers distributed uniformly within the PAAc gel matrix. Upon heating, the dehydration of PPO center blocks takes place, and micellization begins. PPO blocks forming the micellar core together with the entanglements between PEO and PAAc segments act as reversible, breakable crosslinks leading to the increase of the dynamic moduli of IPN hydrogels. At higher AAc contents, associations between PPO blocks

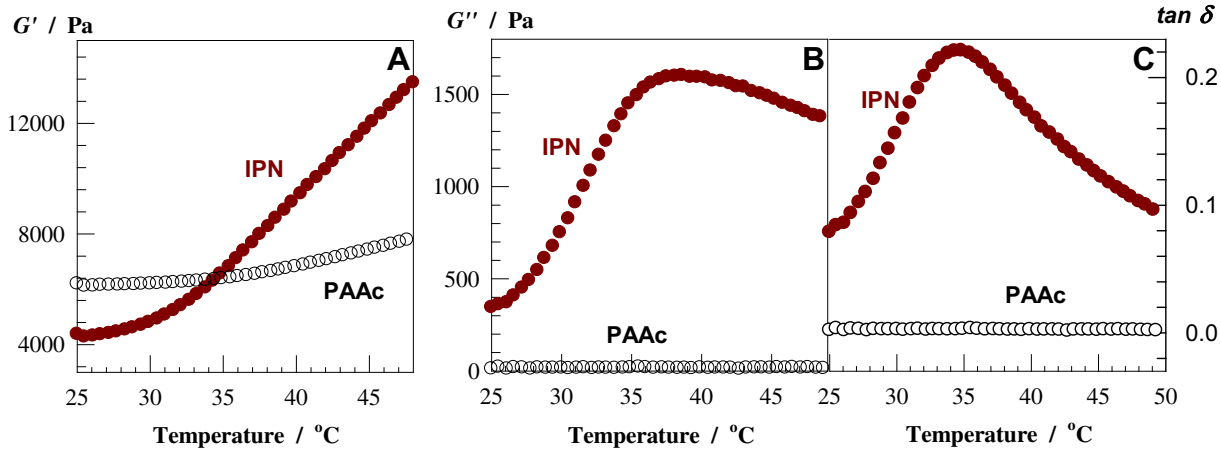

Fig. 7. G' (A) and G'' (B) and tan δ (C) of IPN and PAAc hydrogels during heating from 25 to 50 °C. AAc = 10 w/v%. $\omega = 1$ Hz. $\gamma_o = 0.01$.

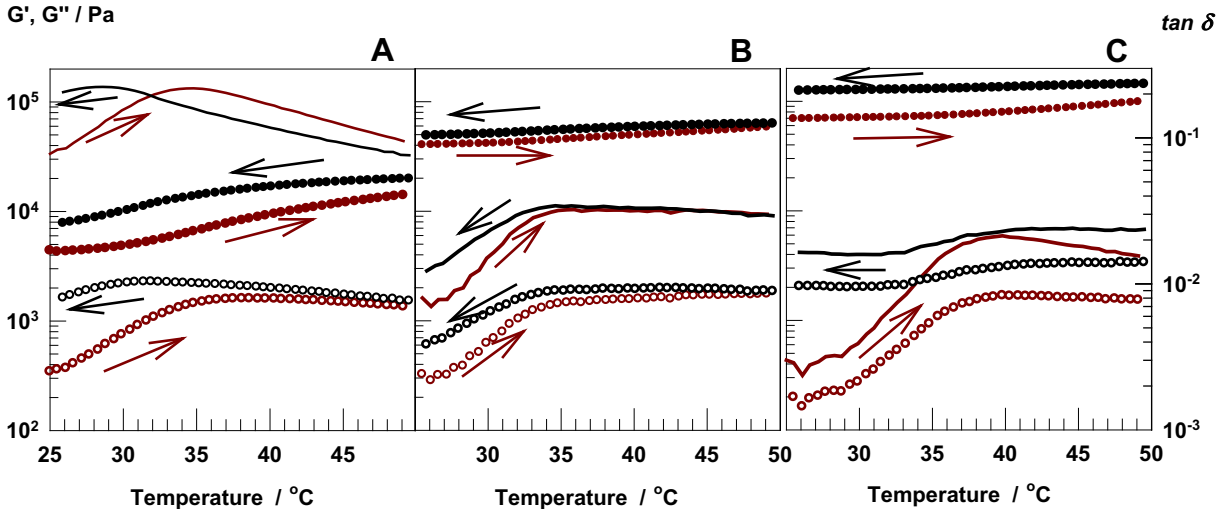

Fig. 8. G' (filled symbols), G'' (open symbols) and tan δ (curves) during the heating/cooling cycle of IPN hydrogels. AAc content in the feed = 10 (A), 20 (B), and 30 w/v% (C). $\omega = 1$ Hz. $\gamma_o = 0.01$. Arrows show direction of the temperature change.

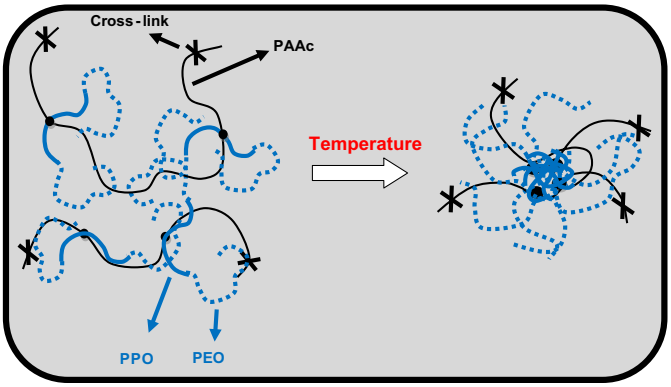

Fig. 9. Cartoon demonstrating conformational change of F127 during heating of IPN hydrogels. Dashed and solid blue curves represent PEO and PPO blocks of F127, respectively, solid black curve represents PAAc network chain and crosses denote chemical crosslinks. (For interpretation of the references to color in this figure legend, the reader is referred to the web version of this article.)

of F127 within the mesh of IPN hydrogels lead to the observed temperature sensitivity.

4. Conclusions

Free-radical crosslinking copolymerization of AAc and BAAm was carried out in 20 w/v% aqueous F127 solutions in the presence of APS-SMS redox initiator system. The crosslinker ratio was fixed at 1/50 while the initial monomer (AAc) concentration was varied between 5 and 30 w/v%. The presence of F127 in the gelation solution slightly decreases the final elastic modulus of the hydrogels while the loss factor significantly increases (from 10^{-3} to 10^{-1}), revealing increasing energy dissipation in IPN hydrogels. Although IPN hydrogels are less crosslinked than PAAc hydrogels, they exhibit a lesser degree of swelling at pH < 9 as compared to the corresponding PAAc hydrogels. This behavior was attributed to the decrease of the dissociation degree of AAc units in the network chains due to the presence of F127 molecules. Comparison of the results of the rheological and mechanical tests show that the associations of F127 within the chemically crosslinked gel network lead to the formation of tough IPN hydrogels. For example, PAAc hydrogel formed at 10% AAc fractures under a compression of 0.2 MPa at 78% strain, while the corresponding IPN hydrogel sustains up to 7 MPa compressions at 98% strain, leading to an increase of toughness from 31 to 335 kJ/m^3. Cyclic compression tests show large mechanical hysteresis in IPN hydrogels due to the reversible formation of ionic clusters and hydrophobic associations of F127 molecules. The larger number of reversibly breakable bonds in IPN hydrogels is responsible for their enhanced mechanical properties. IPN hydrogels subjected to the heating–cooling cycles between below and above the micellization temperature of F127 show characteristic features of F127 solutions, i.e., increase of the dynamic moduli on raising the temperature, and thermal hysteresis behavior.

Acknowledgment

Work was supported by the Scientific and Technical Research Council of Turkey (TUBITAK), TBAG –109T646. O. O. thanks Turkish Academy of Sciences (TUBA) for the partial support.

Appendix A. Supplementary data

Supplementary material associated with this article can be found, in the online version, at http://dx.doi.org/10.1016/j.polymer.2013.03.066.

References

[1] Candau F, Selb J. Adv Colloid Interface Sci 1999;79:149.
[2] Volpert E, Selb J, Candau F. Polymer 1998;39:1025.
[3] Nystrom B, Walderhaug H. J Phys Chem 1996;100:5433.
[4] Wanka G, Hoffmann H, Ulbricht W. Colloid Polym Sci 1990;268:101.
[5] Wanka G, Hoffmann H, Ulbricht W. Macromolecules 1994;27:4145.
[6] Oh KT, Bronich TK, Kabanov AV. J Control Release 2004;94:411.
[7] Lau BK, Wang Q, Sun W, Li L. J Polym Sci Part B: Polym Phys 2004;42:2014.
[8] Alexandridis P, Hatton TA. Colloids Surf A: Physicochem Eng Aspects 1995;96:1.
[9] Prud'homme RK, Wu G, Schneider DK. Langmuir 1996;12:4651.
[10] Meznarich NAK, Love BJ. Macromolecules 2011;44:3548.
[11] Huynh CT, Nguyen MK, Lee DS. Macromolecules 2011;44:6629.
[12] Hoare TR, Kohane DS. Polymer 2008;49:1993.
[13] Klouda L, Mikos AG. Eur J Pharm Biopharm 2008;68:34.
[14] Nam JA, Al-Nahain A, Hong S, Lee KD, Lee H, Park SY. Macromol Biosci 2011;11:1594.
[15] Pruitt JD, Husseini G, Rapoport N, Pitt WG. Macromolecules 2000;33:9306.
[16] Missirlis D, Hubbell JA, Tirelli N. Soft Matter 2006;2:1067.
[17] Wu C-J, Gaharwar AK, Chan BK, Chan BK, Schmidt G. Macromolecules 2011;44:8215.

[18] Sosnik A, Cohn D. Biomaterials 2004;25:2851.
[19] Cho KY, Chung TW, Kim BC, Kim MK, Lee JH, Wee WR, et al. Int J Pharm 2003;260:83.
[20] Gong JP, Katsuyama Y, Kurokawa T, Osada Y. Adv Mater 2003;15:1155.
[21] Haque Md A, Kurokawa T, Gong JP. Polymer 2012;53:1805.
[22] Myung D, Koh W, Ko J, Hu Y, Carrasco M, Noolandi J, et al. Polymer 2007;48:5376.
[23] Harrass K, Krüger R, Möller M, Albrecht K, Groll J. Soft Matter 2013;9:2869.
[24] Stafford JW. Makromol Chem 1970;134:71.
[25] Bromberg L. J Phys Chem B 1998;102:1956.
[26] Bromberg L. J Phys Chem B 1998;102:10736.
[27] Bromberg L. Macromol Rapid Commun 1998;19:467.
[28] Bromberg L, Temchenko M, Hatton TA. Langmuir 2002;18:4944.
[29] Ma W-D, Xu H, Wang C, Nie S-F, Pan W-S. Int J Pharm 2008;350:247.
[30] Oh Y-J, In I, Park SY. J Ind Eng Chem 2012;18:321.
[31] Gundogan N, Melekaslan D, Okay O. Macromolecules 2002;35:5616.
[32] Flory PJ. Principles of polymer chemistry. Ithaca, NY: Cornell University Press; 1953.
[33] Treloar LRG. The physics of rubber elasticity. Oxford: University Press; 1975.
[34] Okay O, Kurz M, Lutz K, Funke W. Macromolecules 1995;28:2728.
[35] Kim K-S, Park S-J. Colloids Surf B 2010;80:240.
[36] Bromberg L, Temchenko M, Hatton TA. Langmuir 2003;19:8675.
[37] Tuncaboylu DC, Sahin M, Argun A, Oppermann W, Okay O. Macromolecules 2012;45:1991.
[38] Tuncaboylu DC, Argun A, Sahin M, Sari M, Okay O. Polymer 2012;53:5513.
[39] Miquelard-Garnier G, Creton C, Hourdet D. Soft Matter 2008;4:1011.
[40] Miquelard-Garnier G, Hourdet D, Creton C. Polymer 2009;50:481.
[41] Halacheva A, Rangelov S, Tsvetanov C. J Phys Chem B 2008;112:1899.
[42] Topuz F, Okay O. Macromolecules 2008;41:8847.
[43] De Gennes PG. Scaling concepts in polymer physics. Ithaca, NY: Cornell University Press; 1979.